IR and Magnetic Studies of Al^{+3} Substituted Co-Mn-FeO_4 Nano Ferrites

M. M. Langade and D. V. Mane*

Department of Chemistry, Shri Chhatrapati Shivaji College Omerga (M.S) 413606

*dvmane11@gmail.com

Abstract:

The IR spectra shows two main absorption bands ν_1 and ν_2 are characteristics of spinel ferrites. The shape, size and morphology of synthesized sample studied by transmission electron microscopy and scanning electron microscopy indicates agglomerated nano particles in the range of 9-18 nanometer. The magnetic properties like remanent magnetization, magneton number and coercivity is affected with increase in Al^{3+} ion concentration.

1 Introduction

Ferrite materials are important magnetic materials, which have various applications in power conditioning and conversion[1-8]. Due to their distinct magnetic properties, ferrite materials have been widely used to prepare many electromagnetic devices such as inductors, converters, phase shifters and electromagnetic wave absorbers [9],[10].

Since, the temperature dependence of the magneto elastic properties is strongly dependent on the magneto striction and magnetic anisotropy, as well as coercivity, permeability, and chemical composition of the material. As per the literature review these properties appeared excellent with Co-Mn ferrite, therefore in our present study we have kept Co-$MnFeO_4$ as a basic composition for further investigation.

A variety of techniques have been used to prepare ferrite materials of nano-scale including co-precipitation method [11-15], sol–gel process [16-18], glass crystallization [19], the mechanical alloying method [20-22], self-propagation [23-24], microemulsion [25], microwave [26-28], hydrothermal [29], and ultrasound-assisted synthesis [30].

Keeping the importance of Co-Mn ferrite and the need to prepared these samples in nanometer dimensions it was decided to synthesize $CoMn_{1-x}Al_xFeO_4$ (x = 0.0, 0.25, 0.5, 0.75, 1.0) ferrite system. The structural and magnetic changes in the Co-Mn ferrite brought by the Al^{3+} substitution synthesized via sol-gel auto-combustion method is discussed here.

The IR spectra shows two main absorption bands ν_1 and ν_2 are characteristics of spinel ferrites. The shape, size and morphology of synthesized sample studied by transmission electron microscopy and scanning electron microscopy indicates agglomerated nano particles in the range of 9-18 nanometer.

2 Experimental

Sol-gel auto-combustion route was adopted to achieve the homogeneous mixing of the chemical constituents at the atomic scale and better sinterability. AR grade cobalt nitrate ($Co(NO_3)_2 \cdot 3H_2O$), aluminum nitrate

($Al(NO_3)_3 \cdot 9H_2O$), manganese nitrate ($Mn(NO_3)_2 \cdot 6H_2O$),iron nitrate ($Fe(NO_3)_3 \cdot 9H_2O$) and citric acid ($C_6H_8O_7 \cdot H_2O$),were used to prepare the $CoMn_{1-x}Al_xFeO_4$ (x = 0.0, 0.25, 0.5, 0.75, 1.0) ferrite compositions. Reaction procedure was carried out in air atmosphere without protection of inert gases. The molar ratio of metal nitrates to citric acid was taken as 1:3. The metal nitrates were dissolved together in a minimum amount of double distilled water to get a clear solution. An aqueous solution of citric acid was mixed with metal nitrates solution, then ammonia solution was slowly added to adjust the pH at 7. Then the solution was heated to 90 ºC to transform it into gel. When ignited at any point of the gel, the dried gel burnt in a self-propagating combustion manner until all gels were completely burnt out to form a fluffy loose powder. The auto-combustion was completed within a minute, yielding the brown-colored ashes termed as a precursor. Finally, the as prepared ferrite powder was annealed at 600 ºC for 4 h. in order to compete the crystallization.

3 Results and discussion

3.1 Infrared spectroscopy

The IR spectra in the range of 200 to 1000 cm^{-1}at room temperature are shown in Fig. 1. The band positions are listed in Table 1.The two wide bands ν_1 and ν_2 are characteristic of spinel ferrites, where their existence reveals that these samples are a single- phase spinel ferrites.

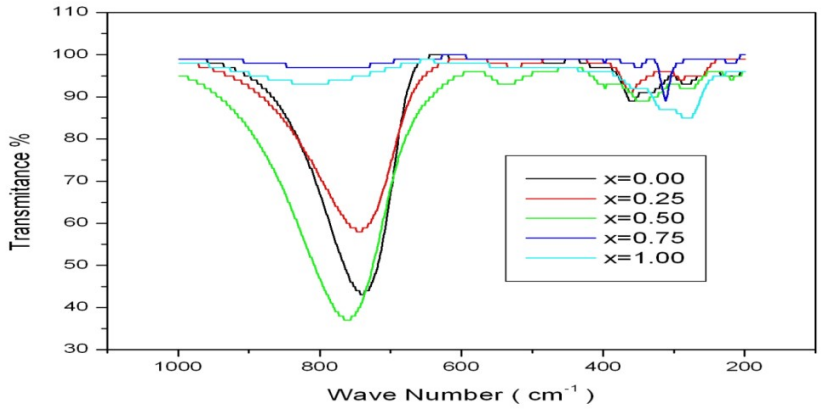

Fig. 1 Infrared spectra of $CoMn_{1-x}Al_xFeO_4$

The band ν_1 lies in the range742 cm^{-1} to 816 $cm^{-1}$and is assigned to the complexes Fe^{3+}–O^{2-}on the A-sites and ν_2 lies in the range of 299 cm^{-1} to 364 $cm^{-1}$and is assigned to Fe^{3+}–O^{2-}on the B-sites vibration modes [33]. The difference in the position of the two strong bands ν_1 and ν_2 could be related to the difference in Fe^{3+}–O^{2-}distance for A-sites and B-sites. It was found that Fe–O distance of A-site (0.189 nm) is smaller than that of the B-site (0.199 nm). The band ν_3 appeared around 527-550 cm^{-1} can be attributed to the divalent metal oxygen complexes Fe^{3+}–O^{2-}, Co^{3+}–O^{2-} and Mn^{3+}–O^{2-} on the A-sites. The band ν_4 appeared around 229-283cm^{-1}may be assigned to the lattice vibrations of the system and is dependent on the A-site complexes Fe^{3+}–O^{2-}, Co^{3+}–O^{2} , [34-35]. The existence of Fe^{2+}ions amongst the sub lattice causes a splitting of its band producing ν_3 at $\nu_1$and ν_4 at ν_2. This results from the distortion of the Jan-teller effect of Fe^{2+}ions [36-37]. TheFe^{2+} ions may result from the hopping process; $Co^{2+}+Fe^{3+} \leftrightarrow Co^{3+}+Fe^{2+}$, $Mn^{2+}+Fe^{3+} \leftrightarrow Mn^{3+}+Fe^{2+}$ where Co^{3+} may migrate into the A-sites and Fe^{2+}ions remains in

their sites.

3.2 Magnetization

Magnetic hysteresis loops for$CoMn_{1-x}Al_xFeO_4$with a maximum applied field of 0.9 T is shown in Figs. 2.All data of the magnetization parameters are included in Table 1 .The values of saturation magnetization (Ms) is appeared to be lower as compared to that of bulk values of Co-Mn ferrite.

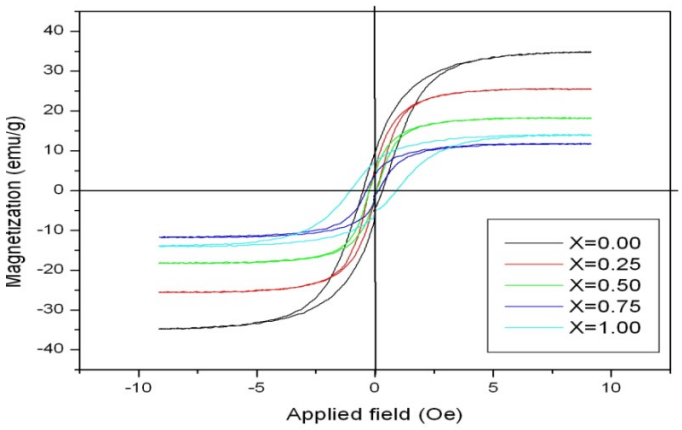

Fig. 2. variation of magnetization (M) with applied magnetic field (Oe) of $CoMn_{1-x}Al_xFeO_4$

Comp. x	υ_1 (cm^{-1})	υ_2 (cm^{-1})	υ_4 (cm^{-1}) υ_3 (cm^{-1})	Ms (emu/g)	M_r (emu/g)	R	η_B (μ_B) Obs.	η_B (μ_B) Cal.	Hc (Oe)
0.00	742	358	533	34.63	9.57	0.28	1.45	3.40	510
0.25	746	364	527	25.28	5.34	0.21	1.03	2.20	224
0.50	763	349	539	17.87	4.61	0.26	0.70	0.80	248
0.75	787	320	550	13.68	3.88	0.28	0.52	0.20	360
1.00	816	299	534	11.39	7.09	0.62	0.42	0.30	1056

Table. 1 IR absorption bands, Saturation magnetization (Ms), remanence magnetization (Mr), remanenceratio (R), magneton number (η_B) and coercivity (Hc) of $CoMn_{1-x}Al_xFeO_4$

Lower saturation magnetization can be considered as a consequence of the smaller crystallite size, which leads to structural distortion in the external surface. This structural distortion occurs because at the external surface the surface spins have nearest neighbors only on one side and none on the other side (broken exchange bonds)

The variation of saturation magnetization with Al^{3+} substitution decrease of saturation magnetization with the Al^{3+}concentration depends up on the three facts:

(1) In spinel ferrite the saturation magnetization (Ms) depends upon strongest super- exchange coupling (antiparallel coupling) between the tetrahedral A and octahedral B site. The strength of super exchange coupling depends on the bond angles and bond lengths between the cations. The exchange coupling decreases with the decrease of effective bond lengths. In the present samples we have observed from XRD analysis the effective bond lengths. Decrease with the increase of Al^{3+}concentration, which leads to weakening the exchange coupling and hence saturation magnetization decreases.

(2) $Al^{3+}$is a nonmagnetic ion, which does not take part in the exchange interaction to the nearest neighbor ions and hence the saturation magnetization affects with the increase of Al^{3+}concentration.

(3) Porosity affects the magnetization process because the pore works as a generator of the demagnetization field. The pores tend to hinder the free movement of the magnetic walls during the magnetization process [38]. As a consequence, the intensity of the effective magnetic field applied to the material is reduced [39]. Increased density reduces the material's porosity. Therefore, a homogeneous and denser microstructure should favor the flow of the magnetic field through the material, improving its magnetic induction. The increase in porosity of the presently investigated samples with Al^{3+} substitution may also play the role in declining the Ms of $CoMn_{1-x}Al_xFeO_4$spinel ferrite.

The observed variation in the saturation magnetization can also be explained due to the difference in the contributions from the magnetic moment of the substituted ion on the A- and B-sites of the $CoMn_{1-x}Al_xFeO_4$spinel ferrite i.e.

$$n_{Bcal.} = M_B - M_A \qquad 12$$

where, M_B and M_A are the B and A sub-lattice magnetic moments in μ_B, $n_{Bcal.}$ is termed as calculated magnetic moment. In the presently investigated ferrite system, decrease in the $n_{Bcal.}$(Fig. 3) is expected after the substitution of Al^{3+} for Mn^{3+} ions, since $Al^{3+}$is a non-magnetic ion with magnetic moment of $0\mu_B$ as compared magnetic Mn^{3+} ion with a large magnetic moment of $4\mu_B$.

The observed magnetic moment ($n_B$obs.) per formula unit in the Bohr magneton (μ_B) was calculated using a relation, [40]

$$n_{B\,Obs.} = \frac{(Mw) \times (Ms)}{5585} \qquad 13$$

where M_W is molecular weight of the sample and Ms is the saturation magnetization. It is obvious from Fig. 7. The calculated and observed values of the magneton number are in good agreement with each other.

Remanence magnetization (Mr) is also decline (Fig. 4) due to Al^{3+} has no remanence; again since it is a soft magnetic material. So, the remanence magnetization comes from the Co, Mn and Fe ions present in the samples.

Fig. 5. depicts the compositional variation of the ratio of remnant magnetization (Mr) over saturation magnetization (Ms) at room temperature measurement. In other words, this ratio (Mr/Ms) is called squareness ratio or remanence ratio (R). Remanence ratio is a characteristic parameter of the material and is dependent on the anisotropy, indicating the ease with which the magnetization direction is reoriented to the nearest easy axis magnetization direction after the magnetic field is removed. The lower the *R* value is, the more isotropic the material will be. The values of *R* varied from 0.28 (x = 0.00) to 0.62 (x = 1.0) with increasing Al^{3+} substitution. This high remanent ratio is desirable for magnetic recording and memory devices.

Coercivity (Hc) in a ferrite system is known to depend on several parameters such as anisotropy constant, lattice imperfections, internal strains and grain size etc. It can be seen from Fig. 6. The coercivity decreased for x = 0.25, which may be attributed to some extrinsic parameters such as micro structures and large grain size. However, it should be mentioned here that the observed coercivity variation invariably points out that the variation in the net anisotropy in the system due to the presence of Co^{2+} and ions is the dominant mechanism responsible for determining the coercivity parameters. Further it can be concluded that the substitution of Al^{3+}in Co-Mn ferrite changing material to a soft magnetic materials, which means that Al^{3+} has almost no coercivity.

Acknowledgement :

The authors are very much thankful to Head of the Chemistry Dept and Principal, Shri Chhatrapati Shivaji College , Omerga for providing necessary facilities and cooperation during the course of work.

References

1. M.H. Sousa, F.A. Tourinho, J. Depeyrot, G.J. da Silva, M.C.F.L. Lara, J. Phys. Chem.B 105 (2001) 1168–1175.
2. Sagar E. Shirsath, Mahesh L. Mane, Yukiko Yasukawa, Xiaoxi Liu and Akimitsu Morisako, Phys. Chem. Chem. Phys. 16 (2014) 2347-2357.
3. Ali Ghasemi, Sagar E. Shirsath, Xiaoxi Liu, and Akimitsu Morisako, J. Appl. Phys. 109 (2011) 07A507
4. Y.F. Lu, W.D. Song, Appl. Phys. Lett. 76 (2000) 490–492.
5. A. Baykal, N. Kasapogul, Y. Koseoglu, A.C. Basaran, H. Kavas, M.S. Toprak, Cent.Eur. J. Chem. 6 (1) (2008) 125–130.
6. C. Venkataraju, G. Sathishkumar, K. Sivakumar, J. Magn. Magn.Mater. 322(2010) 230–233.
7. Sagar E. Shirsath, Yukiko Yasukawa, Ali Ghasemi, Xiaoxi Liu, and Akimitsu Morisako, J. Appl. Phys. 115 (2014) 17A515.
8. M.R. Bhandare, H.V. Jamadar, A.T. Pathan, B.K. Chougule, A.M. Shaikh, J. Alloys Compd.509 (2011) L113–L118.
9. Alex Goldman, Modern Ferrite Technology, 2nd ed. (Springer, New York, 2006).
10. Zhijian Peng, XiuliFu, HuilinGe, ZhiqiangFu, ChengbiaoWang, LonghaoQi, HezhuoMiao, Effect ofPr^{3+}doping onmagneticanddielectricproperties of Ni–Znferritesby‘‘one-stepsynthesis’’ J.Magn.Magn.Mater. 323 (2011) 2513–2518
11. D.H. Chen, Y.Y. Chen, Mater. Res. Bull. 37 (2002) 801–810.
12. S. M. Patange, Sagar E. Shirsath, G. S. Jangam, K. S. Lohar, S. S. Jadhav, K. M. Jadhav, J. Appl. Phys. 109 (2011) 053909
13. V. Uskokovi´ c1, D. Makovec, M. Drofenik, Mater. Sci. Forum 494 (2005) 155–160.
14. Z.F. Zi, Y.P. Sun, X.B. Zhu, Z.R. Yang, J.M. dai, W.H. Song, J. Magn. Magn.Mater.320 (2008) 2746–

2751.
15. M.M. Hessien, M.M. Rashad, K. El-Barawy, J. Magn. Magn.Mater. 320 (2008)336–343.
16. Sagar E. Shirsath, R. H. Kadam, S. M. Patange, M. L. Mane, Ali Ghasemi, Akimitsu Morisako, Appl. Phys.Lett.100 (2012) 042407.
17. Y. Wang, Q. Li, C. Zhang, H. Jing, J. Alloys Compd. 467 (2009) 284–287.
18. Y. Wang, Q. Li, C. Zhang, B. Li, J. Magn. Magn.Mater. 321 (2009) 3368–3372.
19. H. Sato, T. Umeda, J. Mater. Trans. 34 (1993) 76–81.
20. J. Ding, W.F. Miao, P.G. McCormick, R. Street, J. Alloys Compd. 281 (1998) 32–36.
21. W.A. Kaczmarek, B. Idzikowski, K.H. Muller, J. Magn. Magn.Mater. 177 (1998)921–922.
22. S.V. Ketov, Y.D. Yagodkin, A.L. Lebed, Yu.V. Chernopyatova, K. Khlopkov, J. Magn.Magn.Mater. 300 (2006) 479–481.
23. X. Yang, Q. Li, J. Zhao, B. Li, Y. Wang, J. Alloys Compd. 475 (2009) 312–315.
24. L. You, L. Qiao, J. Zheng, M. Jiang, L. Jiang, J. Sheng, J. Rare Earth 26 (2008) 81–84.
25. S. Chaudhury, S.K. Rakshit, S.C. Parida, Z. Singh, K.D.S. Mudhera, V. Venugopal,J. Alloys Compd. 455 (2008) 25–30.
26. Y.P. Fu, C.H. Lin, K.Y. Pan, J. Alloys Compd. 349 (2003) 228–231.
27. Y.P. Fu, C.H. Lin, J. Alloys Compd. 386 (2005) 222–227.
28. F. Tabatabaie, M.H. Fathia, A. Saatchia, A. Ghasemia, J. Alloys Compd. 470 (2009)332–335.
29. J.F. Wang, C.B. Ponton, R. Grossinger, I.R. Harris, J. Alloys Compd. 369 (2004)170–177.
30. I. Perelshtein, N. Perkas, S. Magdassi, T. Zioni, M. Royz, Z. Maor, A. Gedanken, J.Nanopart. Res. 10 (2008) 191–195.
31. B. D. Cullity, Elements of X-ray diffraction, Addison-Wesley, London, 1959.
32. A. R.Denton, N. W.Ashcroft, Phys. Rev. B. 43 (1991) 3161–3164.
33. R.D. Waldron, Phys. Rev. 99 (1955) 1727.
34. M.A. Amer, Phys. Status Solidi B 237/2 (2003) 459.
35. V.I. Nikolaev, V.S. Rusakov, N.I. Chistyakova, Phys. Status Solidi A 91 (1982) K139.
36. V. Potakova, N. Zvera, V. Romanov, Phys. Status Solidi A 12 (1972) 623.
37. H.A. Dawoud, S.K. Shaat, J. Al-Aqsa Univ. 10 (2006) 247.
38. A. Globus, J. Phys. (38) (1977) (C1)1–(C1)15.
39. H. Igarashi, K. Okazaki, J. Am. Ceram. Soc. 60 (1–2) (1976) 51–54.

- ***Paper is submitted for poster presentation at Pre Science Congress 2014 , 30 &31 st December, 2014 at DR. B.A.M. University, Aurangabad***